159

SATELLITE & MESOMETEOROLOGY RESEARCH PROJECT

Department of the Geophysical Sciences
The University of Chicago

WIND SHEAR AT DULLES AIRPORT ON 18 May 1977

by

T. Theodore Fujita

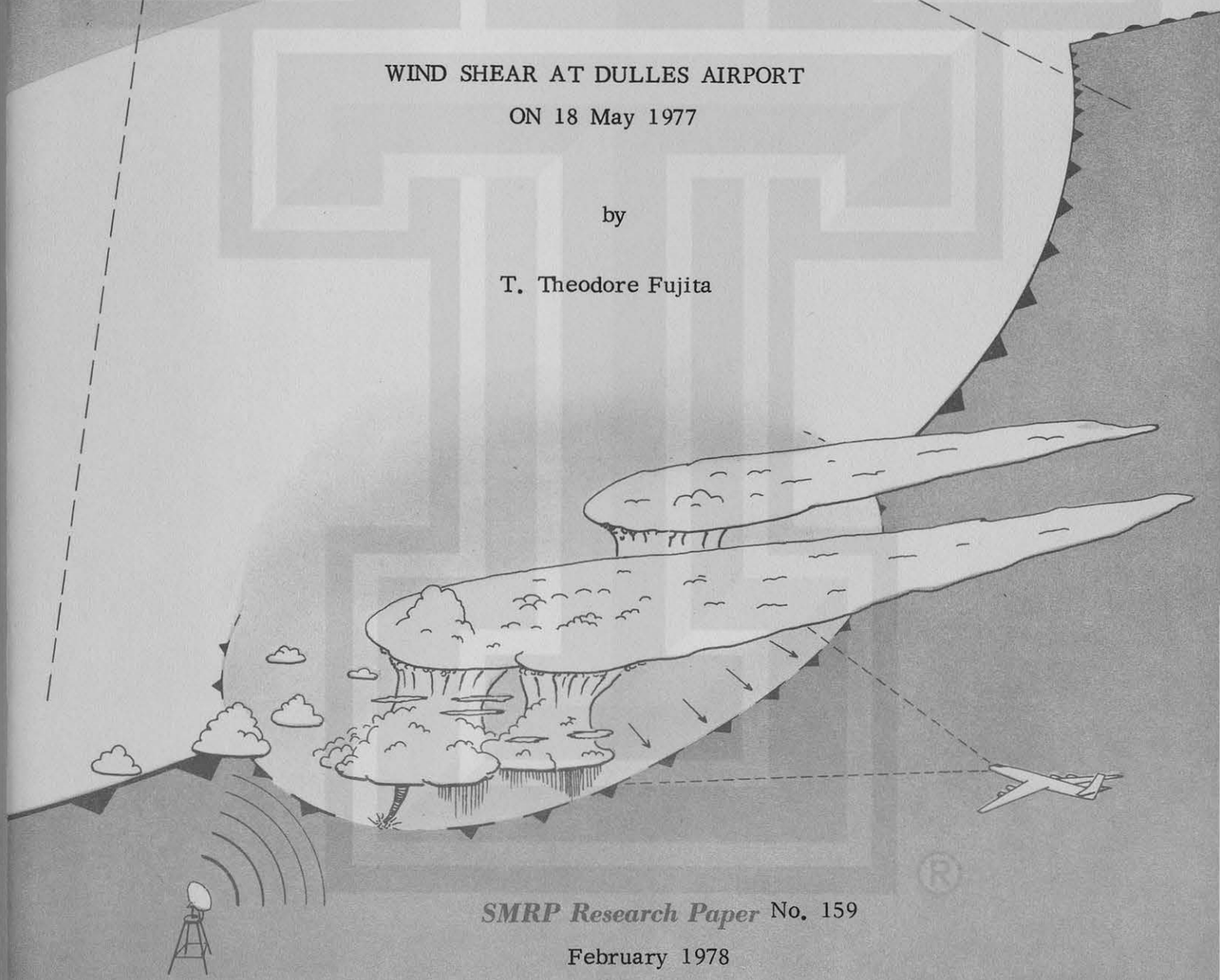

SMRP Research Paper No. 159

February 1978

WIND SHEAR AT DULLES AIRPORT
ON 18 MAY 1977

T. Theodore Fujita
Department of the Geophysical Sciences
The University of Chicago

SMRP Research Paper No. 159
February 1978

Research sponsored by the Wave Propagation Laboratory, ERL, NOAA, Boulder, Colorado.

WIND SHEAR AT DULLES AIRPORT ON 18 MAY 1977

by

T. Theodore Fujita
The University of Chicago

SUMMARY

Meteorological data collected in and around Dulles International Airport on 18 May 1977 were analyzed along with radar pictures from the Patuxent, Md. radar.

Analyses revealed the existence of three types of wind shear which swept across the sensor network. They are "gust-front shear," "behind-the-bulge shear," and "cellular shear."

An array of dP sensors depicted a significant bulge on a gust front. The flow behind the bulge was gusty and strong. A similar gust was depicted when a small air-mass shower moved across the airport area.

The depth of these gusty winds as depicted by an acoustic-microwave radar system at the airport was only about 100 m AGL. The depth of the overall gust front was in excess of 500 m, the limit of the acoustic-microwave radar measurements.

Results of this analysis suggest that the strong wind shear below 100 m is closely related to the outflow from cellular downdrafts/downbursts, either isolated or on a squall line.

I. INTRODUCTION

Various types of wind shear have been determined through use of the wind shear detection system at Dulles International Airport. Of these, three types of shear on May 18, 1977 were depicted and analyzed by the author. They are

CELLULAR WIND SHEAR which is induced by an isolated cell or downdraft. The cell takes the shape of an air-mass shower separated from an organized convected activity.

GUST-FRONT WIND SHEAR which occurs along a long gust front line, often extending over 100 miles along the leading edge of an advancing line of showers.

BEHIND-THE-BULGE WIND SHEAR which is accompanied by an active downdraft cell within a squall line. A portion of the gust front ahead of the cell displays a bulge which moves faster than other portions of the gust front.

The three types of wind shear defined above are presented schematically in Figure 1. The regions of gusty winds are shown by dotted areas. Shear lines are dashed and radar echoes are solid. Arrows extending out from echoes are trajectories of outflow spreading out from their sources.

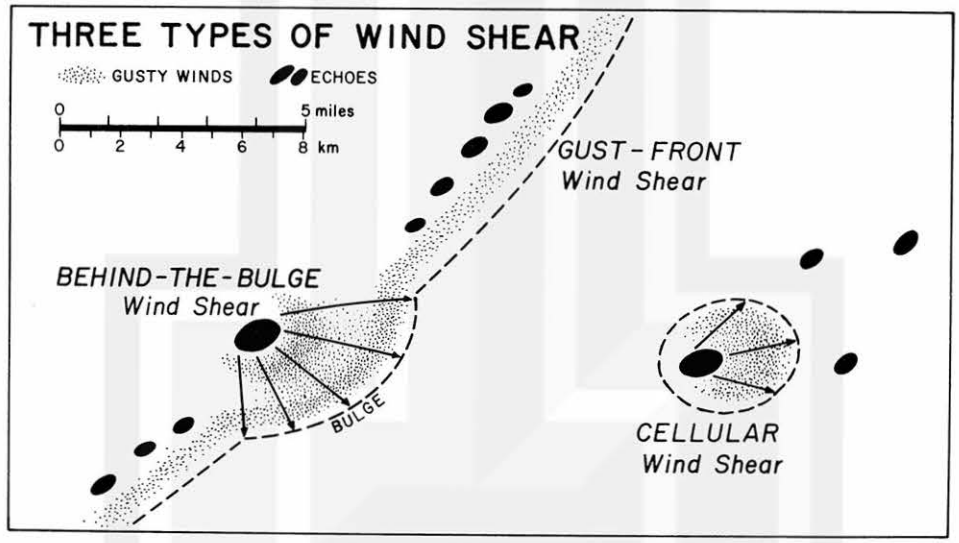

Figure 1. Three types of wind shear depicted over Dulles Airport on May 18, 1977. Shortly after 1900 GMT, cellular wind shear affected the airport. $2\frac{1}{2}$ hours later a gust front swept across the airport.

An example of the flow behind a shear line over the Thunderstorm Project network in Ohio is shown in Figure 2. There was no rain at 1910 EST (left chart). Cold air behind the line was spreading out toward the southeast. In 20 minutes, weak showers developed behind the line. Field of divergence was induced beneath each shower, thus modifying the semi-parallel flow which existed 20-min earlier.

This example reveals that the air flow near the surface can be modified by showers within a very short time. Obviously, each shower, in its downdraft stage, induces a field of divergence which is superimposed upon the overall field of motion behind the shear line. When a shower behind the line is characterized by an unusually large divergence, a bulge on the shear line develops. If a superimposed divergence is small, the shear line advances without showing a visible deformation.

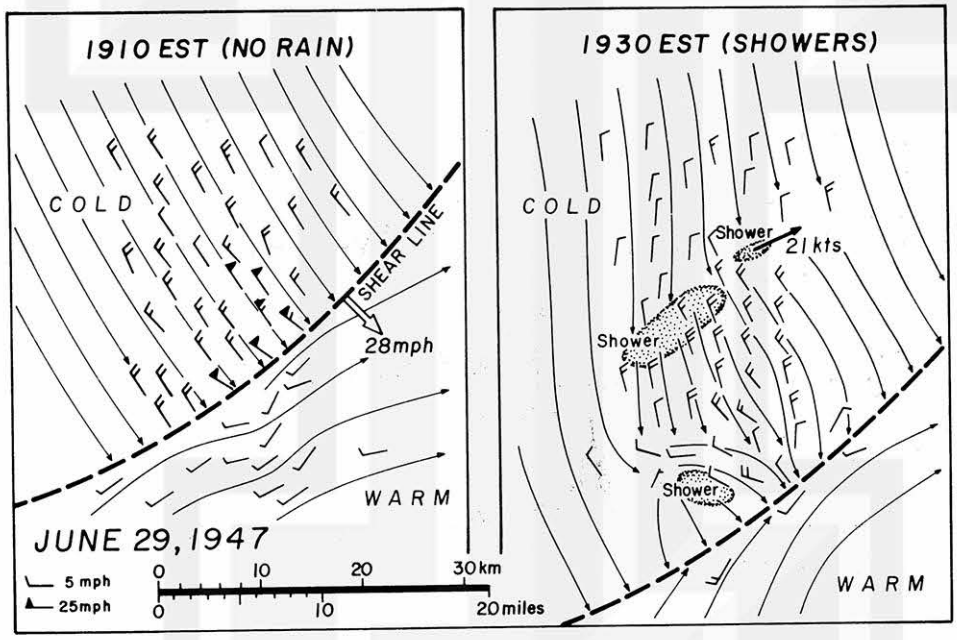

Figure 2. Modification of the flow behind a shear line by showers. During a 20-min period between 1910 and 1930 EST, downdrafts in showers induced divergence fields which were superimposed upon the general flow.

An example of a "cellular wind shear" over the Thunderstorm Project network, Ohio is presented in Figure 3. A downdraft descended over Station 46 resulting in a 0.8 mb pressure rise in 6 min. As the outflow spread out, stations along concentric rings recorded surges of wind up to 33 mph. The wind surge decreased as the distance from Station 46 increased.

Time-sequence analyses reveal that the surge of gusty winds spread out rapidly forming an expanding arc or ring. Peak gusts are seen at two locations; one behind the expanding arc (expanding peak gust) and the other, around the downdraft nadir (off-nadir peak gust). The former or the expanding peak gust weakens as it moves out while the latter or the off-nadir peak gust disappears upon termination of the downdraft.

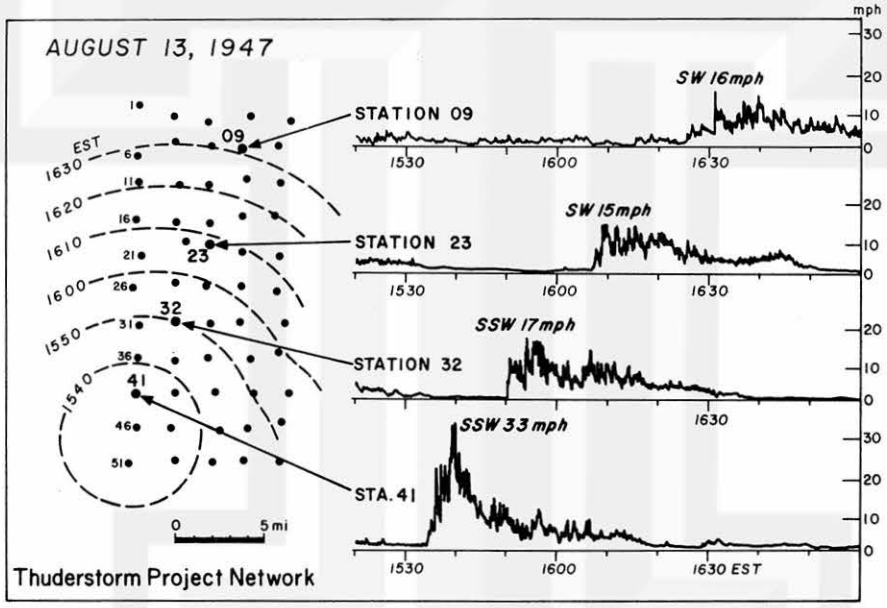

Figure 3. Weakening gusty winds radiating out from a cellular downdraft which descended over Station 46 of the Thunderstorm Project Network.

A numerical simulation of an axisymmetric downdraft by Teske and Lewellen (1977) depicted the features of the double peaks in gust speeds. One example from their experiment showed one peak (1.6 km radius) at 3.3 min., two peaks (1.5 km and 4 km radii) at 8.3 min., and two peaks (1.5 km and 6.3 km radii) at 16.7 min. after flow initialization. Throughout the experimental time steps the speed of the peak at 1.5 km radius (off-nadir peak) was higher than that of the expanding peak.

It is the purpose of this appendix to use mesoanalysis techniques in analyzing meteorological data collected in and around Dulles International Airport.

Basic meteorological data for May 18, 1977 were inspected and supplied by Mr. A. J. Bedard of the Wave Propagation Laboratory, NOAA, at Boulder. Data are

1. Anemometer data. Traces from Stations A1, A2, and the National Weather Service at the airport.
2. dP data. Initial trigger times of dP sensors.
3. Absolute pressure data. Shape of pressure rises which triggered dP sensors.
4. Acoustic-microwave radar data. Wind direction and speed at 30-m intervals up to 510-m height.
5. Monostatic acoustic sounder data.

These materials were used as the basic data in performing this meso-meteorological analysis. Used in addition to these basic data are radar pictures taken at Patuxent River, 70 miles southeast of the airport.

II. CELLULAR WIND SHEAR

A small cellular echo, moving toward the southeast at 30 km/hr, was at the northwest corner of the 10-mile square box around Dulles International Airport. In 20 minutes, the echo moved across the square box affecting the air flow in and around the airport (see Figures 4 and 5).

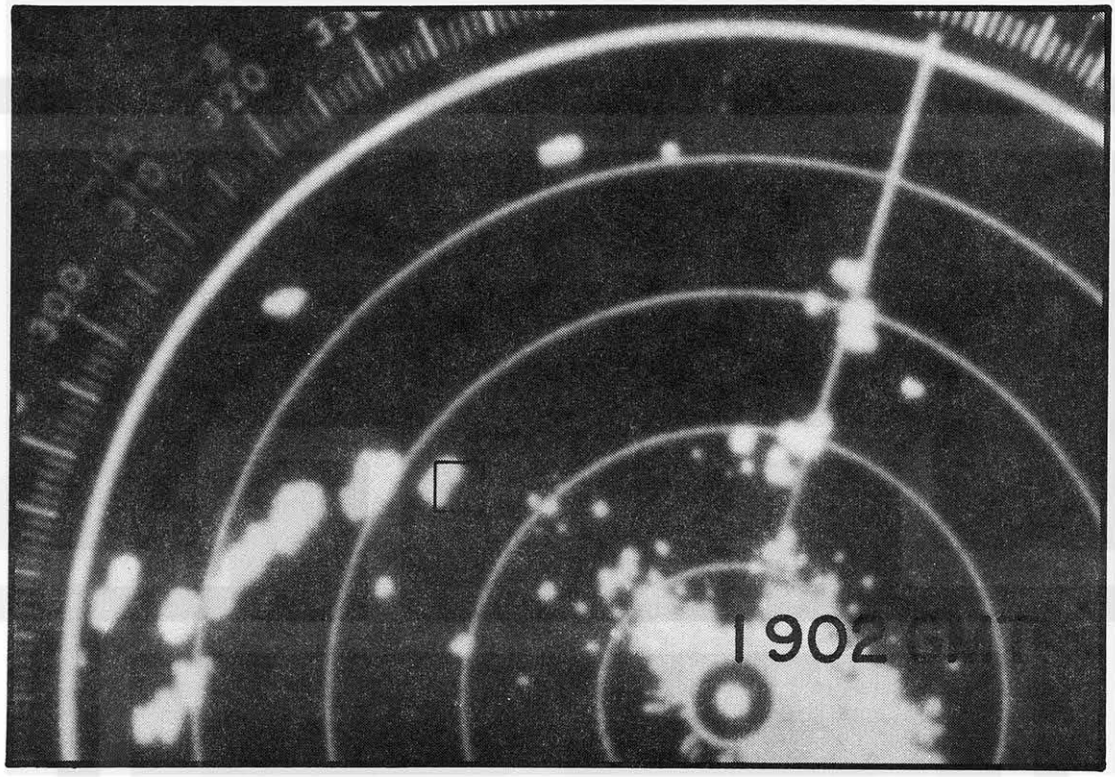

Figure 4. A small cellular echo which had entered the 10-mile square box around Dulles Airport. Time 1902 GMT, 18 May 1977 and range marks are 25 n.m. intervals.

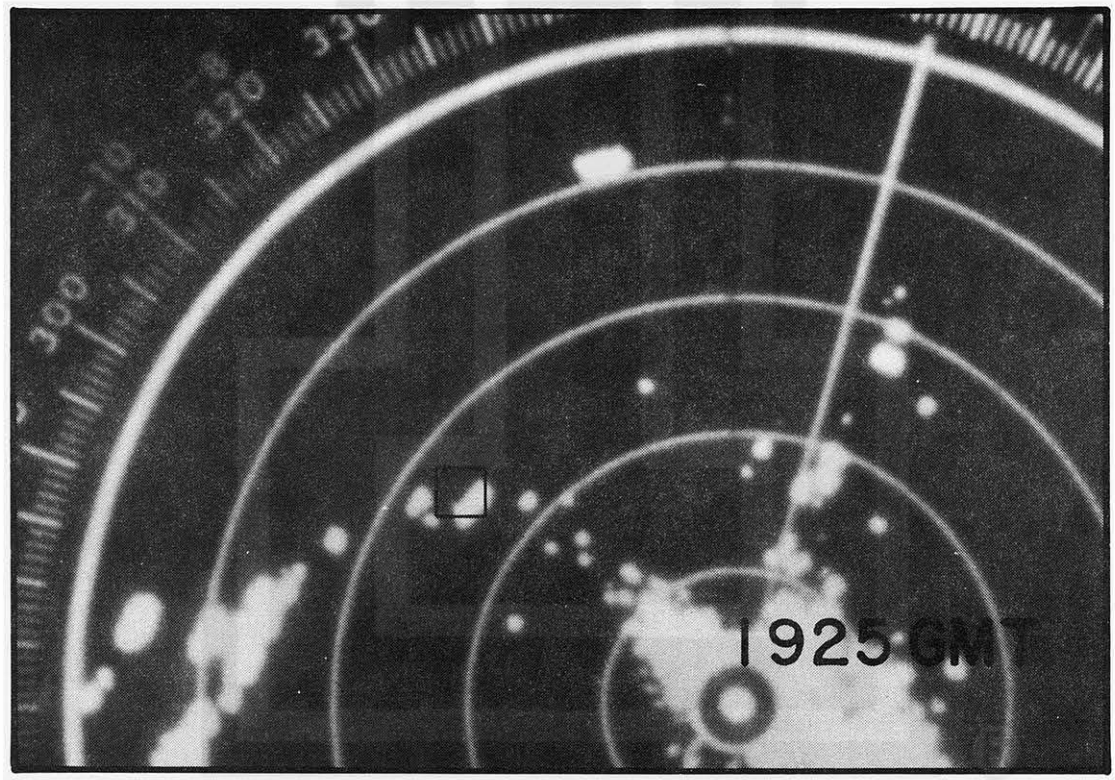

Figure 5. At 1925 the cellular echo reached the southeast corner of the 10-mile square box. The echo was moving from NW to SE at 30 km/hr.

Shown in Figure 6 are the distribution of dP sensors relative to the 10-mile square box around Dulles International Airport. Note that a range of mountains exists to the west of the square box. Eastern sectors from the airport are relatively flat and open all the way to the Atlantic Coast.

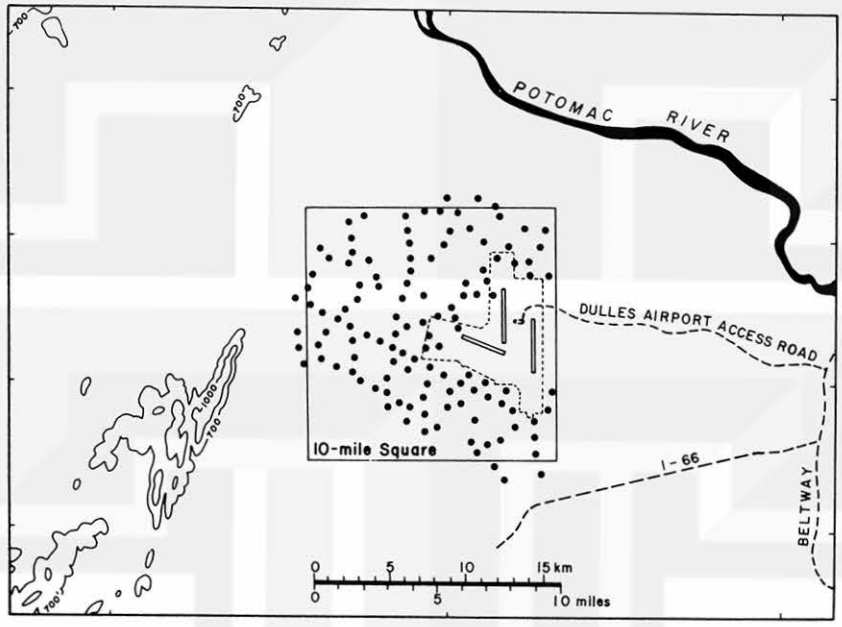

Figure 6. Distribution of dP sensors within the 10-mile square box around Dulles International Airport. Topography around the airport is shown with 700-ft and 1000-ft contour lines. For a description of the dP sensor array, refer to Bedard, Hooke, and Beran (1977).

At first, an attempt was made to estimate the air flow at the anemometer level by converting time variations into space variations. The flow in Figure 7 was, thus, obtained by shifting wind stations at 30 km/hr toward the northwest, opposite from the echo movement.

Wind speeds are expressed by standard barbs, 10 kts for each long barb. Speeds are also contoured by isotachs with 10, 15 and 20 kts. Wind barbs and isotachs reveal that the strongest outflow from the cellular echo over the network was pushing eastward.

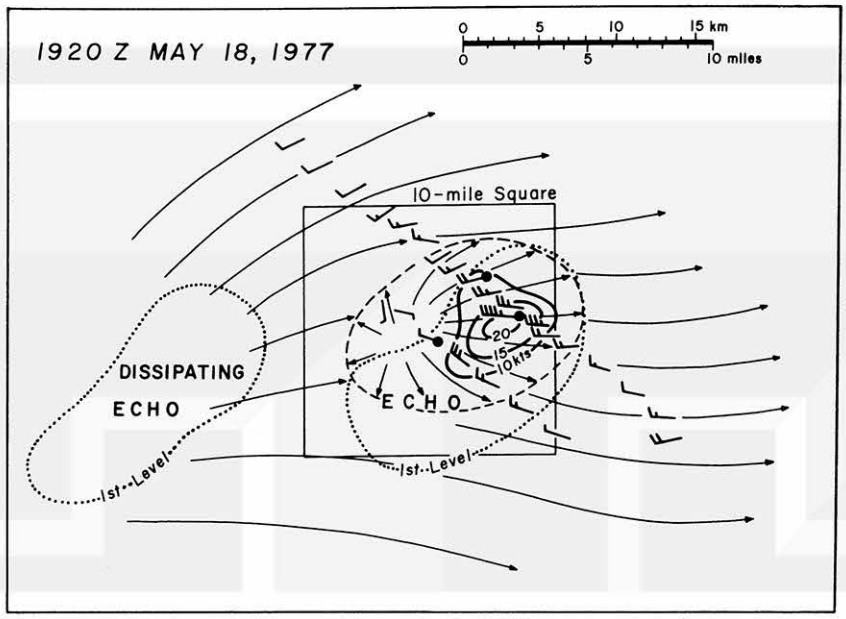

Figure 7. Flow field at the anemometer level estimated by converting time variations into space variations relative to the echo velocity. For time-space conversion techniques for mesoanalysis, see Fujita (1963).

The second diagram in Figure 8 is the trace of the anemometer at the Acoustic-Microwave Radar site. There was a distinct peak gust of 19 kts at 1915 Z. The measurement times of acoustic-microwave radar were at 1911.5 and 1917.5, missing the time of the peak gust by 3.5 and 2.5 min., respectively.

Of extreme interest is the depth of the high-speed outflow. There was a distinct low-speed layer above 100 to 120 m AGL, suggesting strongly that the depth of the strongest outflow was very shallow.

Pressure began rising upon arrival of the outflow and rainfall which occurred at the site during the peak gust time. Air temperature dropped about 10 C in 20 min. and recovered within the next 20 min.

INDEPENDENCE DAY DOWNBURSTS

19 DOWNBURST

40 – 72 mph F0

73 – 112 mph F1

113 – 157 mph F2

0 5 10 15 20 25 30 Miles

0 5 10 20 30 40 50 Kilometers

Aerial Survey and Mapping by T. T. FUJITA on July 13 and 14, 1977

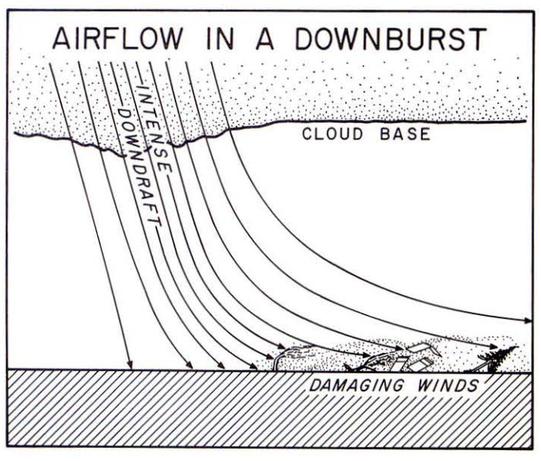

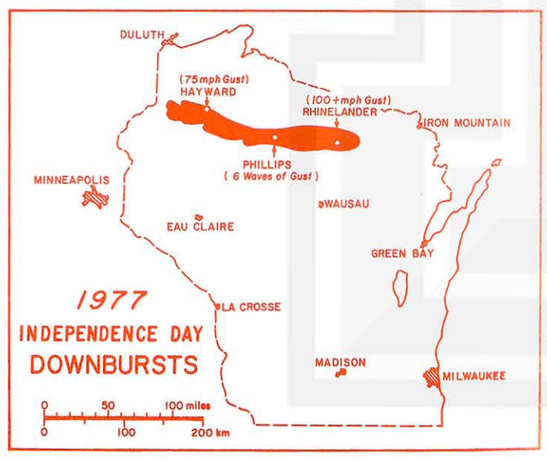

On INDEPENDENCE DAY, the 4th of July 1977, a severe thunderstorm moved across Northern Wisconsin. It was reported that there were extensive areas of tree and property damage, somewhat like that of an oversized tornado.

In cooperation with the National Weather Service Milwaukee Office and the National Severe Storms Forecast Center, Fujita made an aerial survey, mapping both direction and F-scale intensity of damaging winds. No evidence of a tornado was found anywhere inside the damage swath which was 166-mile long and 17-mile wide. Instead, there were scattered local centers from which straight-line winds diverged out violently. These local wind systems were identified as downbursts and numbered 1 through 25.

A downburst, designating downward rush of air current with horizontal outflow, is a downdraft of an extreme intensity accompanied by damaging winds on the ground. Although most downdrafts are not damaging at the surface, a downburst could cause severe damage which was evidenced in Northern Wisconsin on Independence Day.

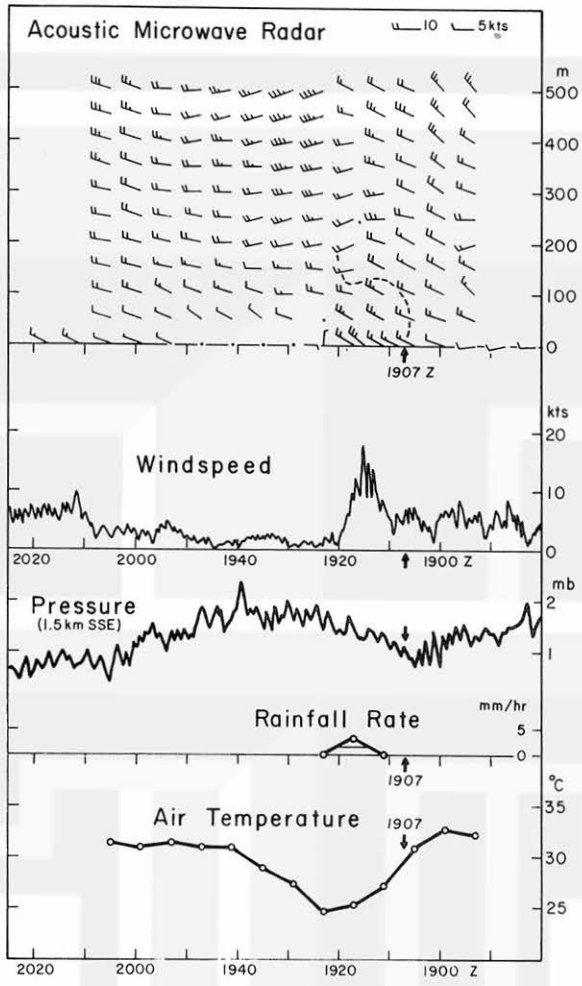

Figure 8. Time variations of winds aloft, speed of surface wind, surface pressure, and air temperature. Note that the strongest outflow is located below the 100-m level. For a description of the acoustic-microwave radar, refer to Hardesty, Mandics, Beran, and Strauch (1977).

Finally, a vertical cross section of winds aloft and surface outflow were combined into a 3-D presentation (see Figure 9). Although the acoustic-microwave radar was located to the south of the maximum gust area (over 28 kts), the vertical distribution of measured wind clearly shows a very shallow outflow depth. It is only about 100 m AGL.

This evidence suggests that the descending air from such an isolated cellular storm can spread out like a shallow jet creeping above the surface. It will be shown later that most aircraft accidents during landing and takeoff phases occurred below 150 m AGL.

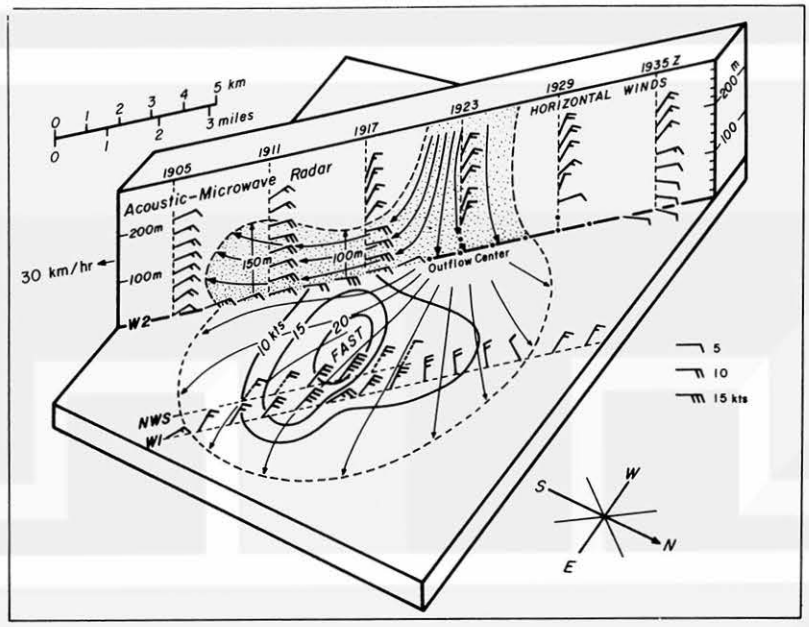

Figure 9. Vertical cross section of cellular outflow over Dulles Airport between 1905 and 1935 Z, 18 May 1977. The acoustic-microwave radar was located to the south of the maximum gust area (over 28 kts).

III. GUST FRONT AND BEHIND-THE-BULGE WIND SHEAR

Gust fronts have been regarded as being an aviation hazard when attempts are made to fly through the fronts at low altitudes. As shown schematically in Figure 1, a gust front extends through a long distance along an arc-shaped line.

At 2222 Z on 18 May 1977, several hours after the cellular wind shear, a long gust front approached Dulles airport from the northwest (see Figure 10).

If the approaching gust front is a long, smooth line, its advancement, as depicted by dP sensors, must be from northwest to southeast across the 10-mile square box.

The actual triggering of dP sensors started in the northern portion of the box and ended near the southwest corner. The isochrones of dP triggers in Figure 11 indicate the propagation of the pressure front from north to south, rather than from northwest to southeast. What was the cause of such an odd propagation?

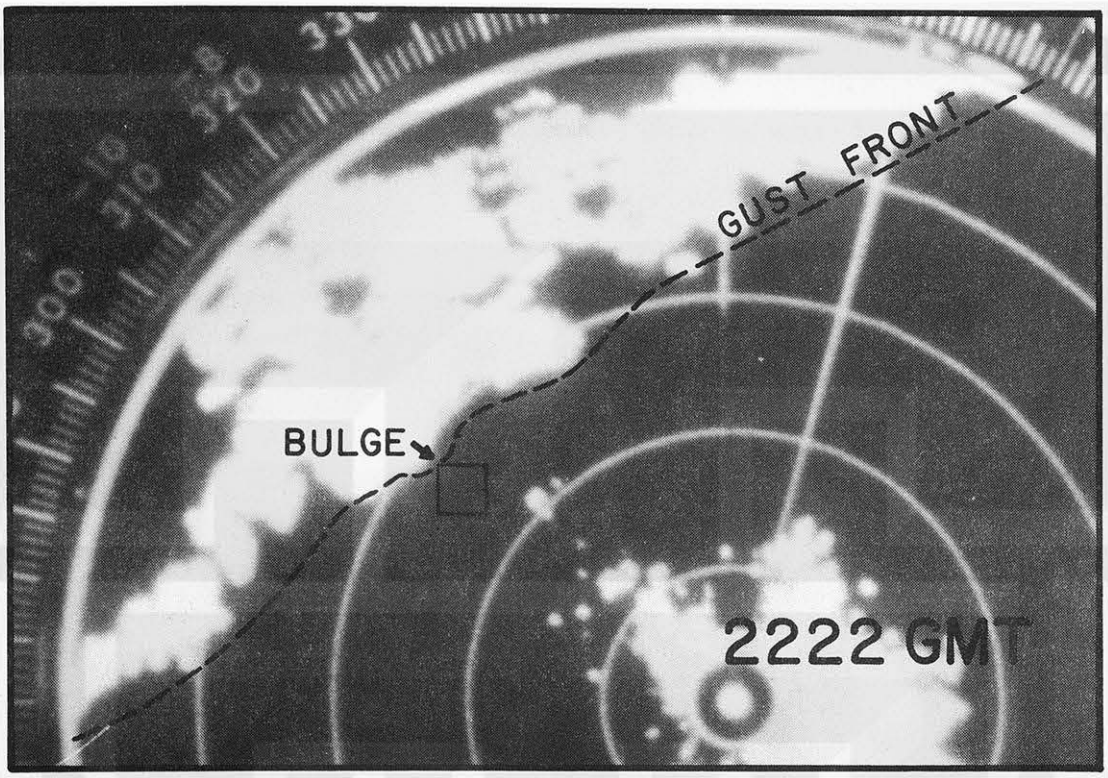

Figure 10. A gust front and line of echoes approaching Dulles airport at 2222 Z, 18 May 1977.

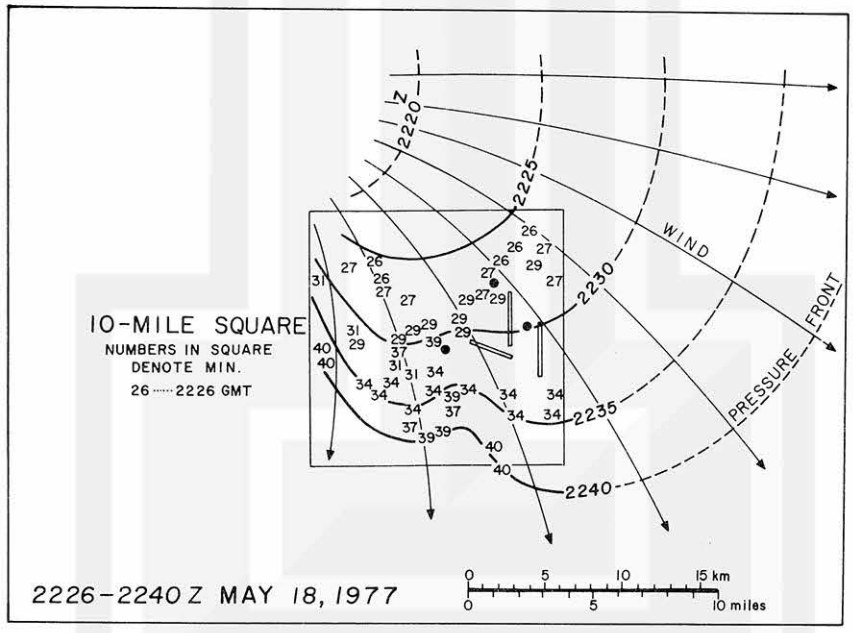

Figure 11. Isochrone of trigger times of dP sensors around Dulles Airport. The two unit numbers at each sensor location denote the time in minutes past 2200 Z, 18 May 1977. Note that isochrones moved from north to south while the parent gust front swept across the airport area from northwest to southeast.

Examination of the 2237 Z picture in Figure 12 reveals that there was a large, strong echo behind the bulge of the gust front. Arrows in the picture denote the direction of expected push (both wind and pressure front) behind the bulge.

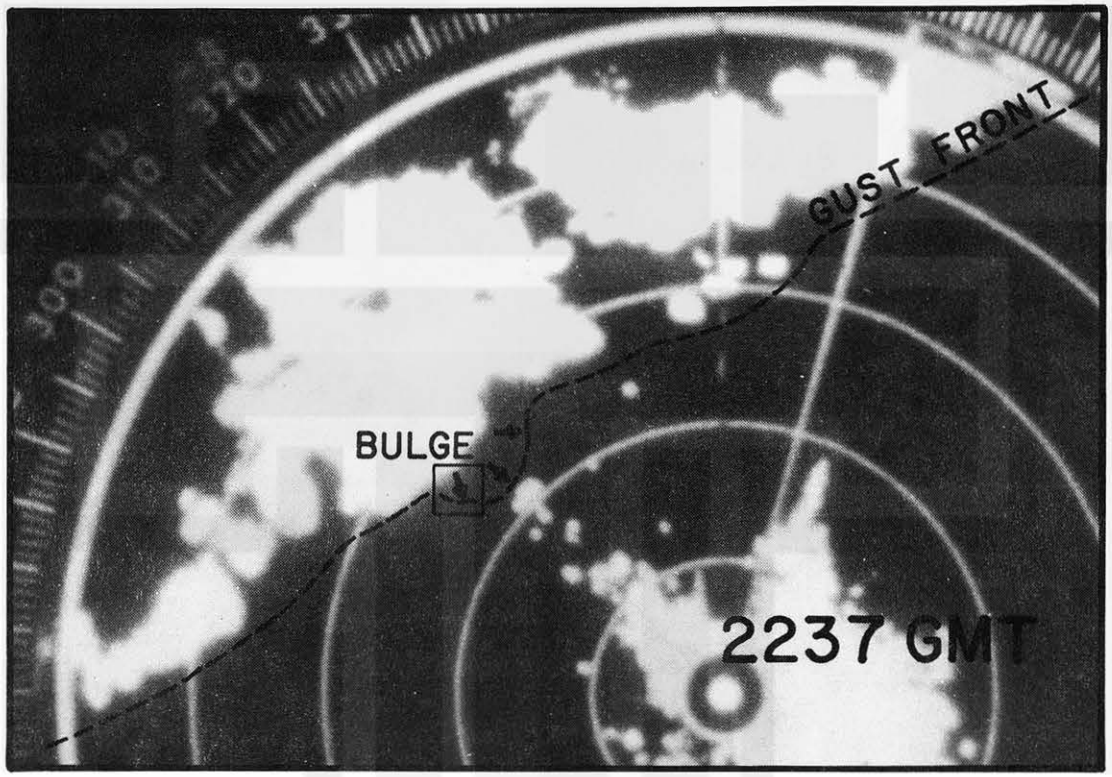

Figure 12. A bulge on the gust front at 2237 Z depicted by isochrones of trigger times of dP sensor. There is a wide, echo-free area between the bulge and a strong echo behind the bulge.

No precipitation echoes are seen between the bulge and the strong echo to the west of the bulge at 2237 Z. In about 30 min., however, a group of small echoes developed behind the bulge. They amalgamated into a large mass of echoes by 2324 Z (see Figure 13).

Development of echoes behind the bulge suggests the existence of a surge of cold air which induced the so-called "plowing effect".

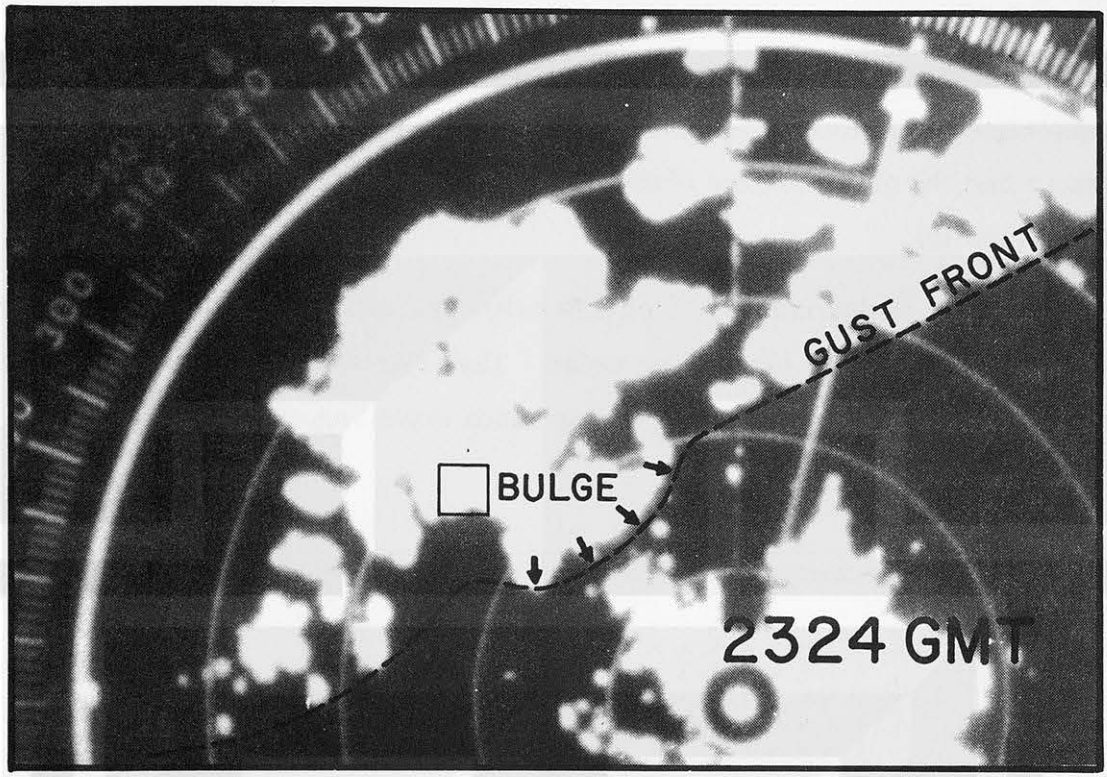

Figure 13. Less than one hour later at 2324 Z, a group of echoes formed just behind the bulge, suggesting that the plowing action of the cold air behind the bulge gave rise to the echo development inside the echo-free area at 2237 Z.

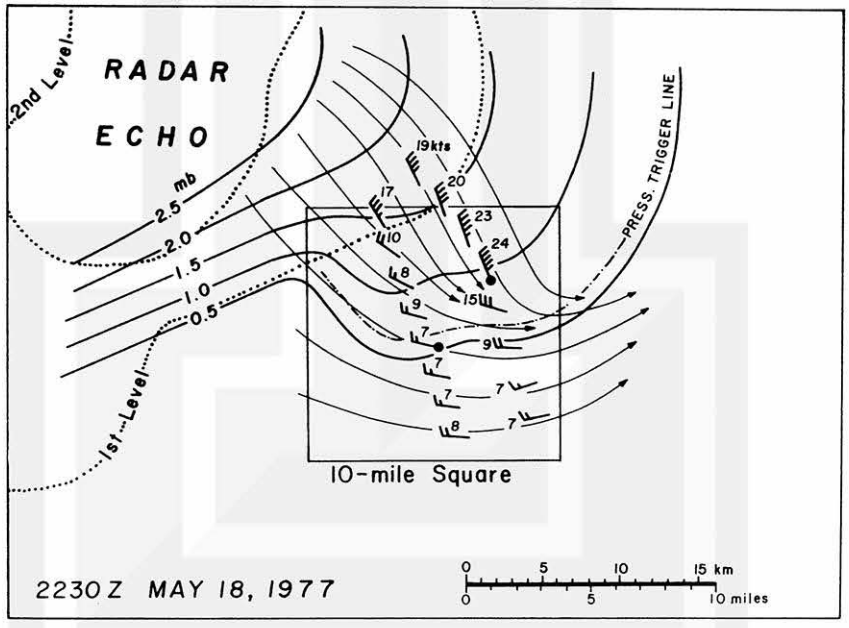

Figure 14. Airflow near the ground on both sides of the pressure trigger line at 2230 Z, 18 May 1977. It is seen that a strong outflow which induced the bulge came from a large echo with level 2+ intensity.

Time-space conversion of surface winds presented in Figure 14 shows clearly that there was a strong outflow behind the pressure trigger line. The wind direction was, more or less, perpendicular to the bulge. It is reasonable to assume that the major source of the outflow was the large radar echo with level 2+ intensity.

The depth of the outflow behind this bulge was depicted beautifully by winds measured by the acoustic-microwave radar. The vertical cross section of winds in Figure 15 shows that there were plowing winds extending to about 100 m AGL.

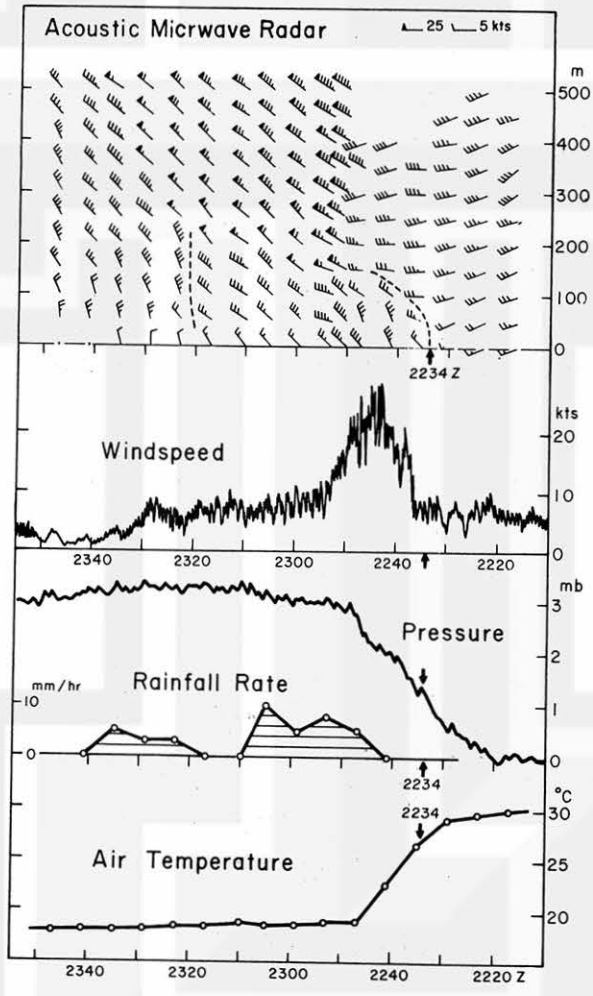

Figure 15. Acoustic-microwave radar winds showing the depth of the outflow behind the bulge to be only about 100 m. It should be noted that the gusty winds near the surface between 2235 and 2250 Z (about 15 min) occurred behind the bulge of the gust front. Main precipitation between 2240 and 2310 Z occurred when the bulge-inducing cell moved over the site.

The plowing winds began at 2234 Z, reaching their peak at 2242, and died out by 2255 Z. The wind direction at the peak was from north-northwest which is perpendicular to the bulge depicted by the isochrone of the pressure trigger line.

It is extremely likely that the outflow from the level 2+ cell on the squall line induced this plowing wind which extended to about 100 m in depth. The plowing winds are, in effect, superimposed upon the overall gust front which extended over 100 miles in a WSW-ENE direction.

Apparently, the depth of the west-northwest wind perpendicular to the overall gust front was in excess of 500 m, the upper limit of the acoustic-microwave sensor measurements. It is unlikely that the wind surge at the high levels associated with a large-scale gust front is closely related to the gusts of plowing winds near the surface. Consequently, wind surge at high levels may move over the airport without inducing significant gusts below 100 m AGL.

Stability of the atmosphere near the ground could easily generate a "shielding effect" of the wind surge due to a long and old gust front. There are numerous cases in which pressure jumps are not associated with either wind surges or temperature drops near the surface, especially at night.

IV. SCALES OF CELLULAR WIND SHEAR ASSOCIATED WITH AIRCRAFT ACCIDENTS AND PROPERTY LOSSES

It is still difficult to unambiguously pinpoint the direct causes of aircraft accidents and property damage in convective storms. Two mesoscale wind systems involved are likely to be

(a) Overall gust front in advance of a squall line extending tens of miles. The depth of the flow behind the front is relatively deep, often accompanied by a roll or a wall cloud.

(b) Cellular outflow induced by a downdraft cell. The horizontal dimensions in its active stage are only up to several miles. The depth of the outflow is only about 100 m.

Based on the analyses of several accident cases and aerial surveys of damage patterns, the author believes that cellular wind shear has been causing more damage than overall gust front wind shear.

Shown in Figure 16 is a stormy-looking roll cloud about 10 miles to the north of the major band of downburst. Vacationers watched the cloud coming toward them and took cover prior to the passage of the cloud.

Unexpectedly, they said, "the cloud passed overhead with a few sprinkles of rain and 10 to 15 mph winds lasted only 2 to 3 minutes."

A roll cloud often could be more violent than this. Nevertheless, this type of cloud or wind shear can be detected, and warning given, by virtue of its large dimensions and long life.

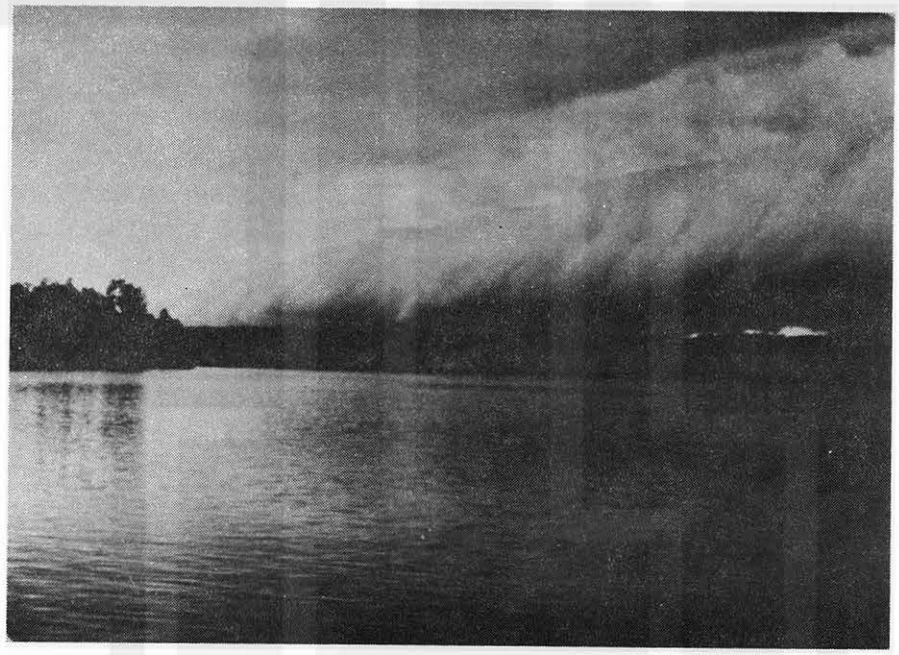

Figure 16. Stormy appearance of a roll cloud during the Northern Wisconsin downbursts of July 4, 1977. This photo was taken by Mrs. G. W. Reid about 10 miles to the north of the downburst band (see color map attached). Everybody ran for cover, but the cloud passed over the area with sprinkles of rain and the 10 to 15 mph wind lasted 2 to 3 minutes.

Cellular outflow induced by a downdraft cell, (b), is smaller than the overall gust front in advance of a squall line, (a), and its life is only 5 to 10 minutes. Furthermore, its outflow winds are strong below about 100 m AGL. Yet, the parent cellular echo is quite often "innocent looking".

Shown in Figure 17 are horizontal dimensions of cellular outflows contributed to aircraft accidents and property losses. Each one of these outflows was less than 5 miles across, but the horizontal size was large enough to result in the strong wind shear during landing and takeoff phases of jet aircraft.

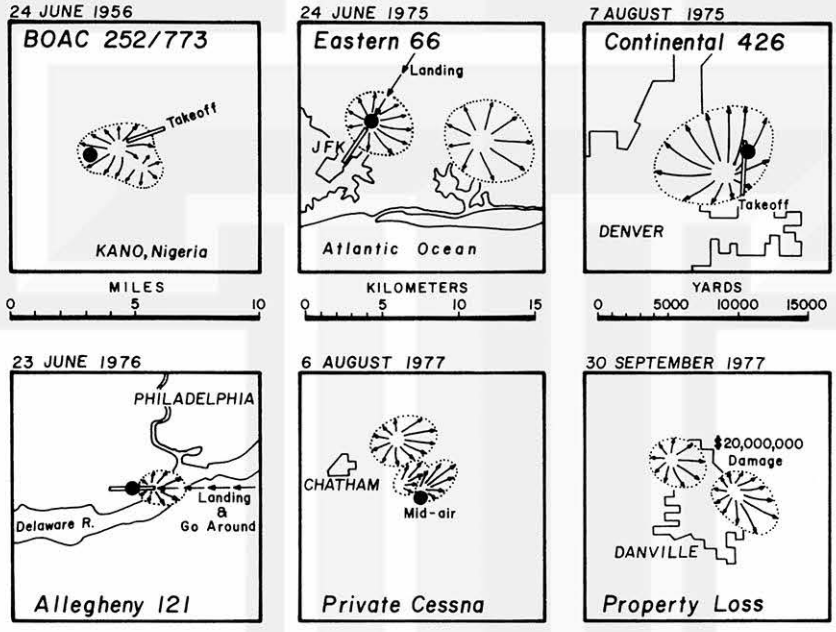

Figure 17. Horizontal dimensions of cellular downbursts which caused aircraft accidents and property losses. To normalize dimensions, downbursts were mapped within 10-mile square boxes. See references to identify data sources.

When the flight paths are drawn in a composite manner relative to the downburst flow in Figure 18, we see that all aircraft encountered difficulties while flying below 100 m AGL. At such an altitude, maneuvering of the aircraft in a flap-down position would be extremely difficult unless an advance warning were transmitted to the pilot.

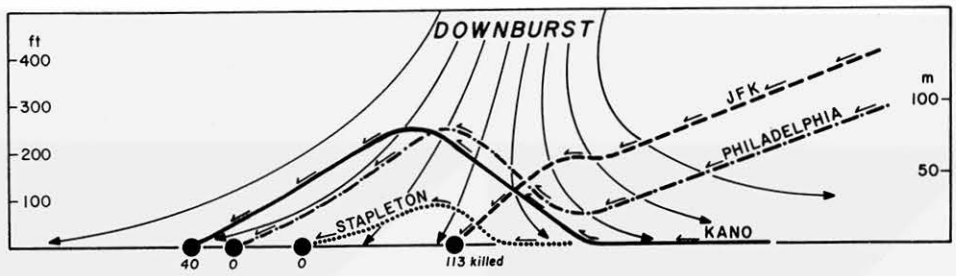

Figure 18. Vertical cross section of the paths of four aircraft which crashed in downbursts. In all four cases aircraft maneuvered desperately below 100 m AGL. Acoustic-microwave radar winds in Figures 8 and 15 measured an effective depth of cellular and behind-the-bulge wind shear of about 100 m.

V. CONCLUSIONS

The results of the data analysis have revealed the unique capabilities of the Dulles multi-sensor, wind-shear detection system. This one-of-a-kind measuring system has already provided valuable insight into the generation and evolution of low-level wind shear at an operational airport. The collection and analysis of additional data at Dulles will substantially increase our understanding of wind shear and the hazards it presents to aviation.

ACKNOWLEDGEMENT:-

Research sponsored by the Wave Propagation Laboratory, ERL, NOAA, Boulder, Colorado.

REFERENCES

ALLEGHENY 121 on 23 June 1976 by F. Caracena (1976). "Mesoscale Features involved in the crash of Allegheny Flight 121 at Philadelphia on June 23, 1976." Report to NTSF. 8 pp.

Bedard, A. J., Jr., W. H. Hooke and D. W. Beran (1977): The Dulles Airport Pressure Jump Detector Array for Gust Front Detection. Bull. of AMS, 58, 920-926.

CONTINENTAL 426 on 7 August 1975 by T. T. Fujita and F. Caracena (1977). "An Analysis of Three Weather-Related Aircraft Accidents. Bull. of AMS, 58, 1164-1181.

EASTERN 66 on 24 June 1975 by T. T. Fujita and H. R. Byers (1977): Spearhead Echo and Downburst in the Crash of an Airliner. Mon. Wea. Rev., 105, 129-146.

Fujita, T. T. (1963): Analytical Mesometeorology. Met. Monographs, 5, 77-125.

Hardesty, R. M., P. A. Mandics, D. W. Beran, and R. G. Strauch (1977): The Dulles Airport Acoustic-Microwave Radar Wind and Wind Shear Measuring System. Bull. of AMS, 58, 910-918.

Teske, M. E. and W. S. Lewellen (1977): Turbulent Transport Model of a Thunderstorm Gust Front. Preprints, AMS 10th Severe Local Storms Conf., 143-150.